Temperature-sensitive mechanical properties of GFRP composites in longitudinal and transverse directions: A comparative study

Allan Manalo[1], Ginghis Maranan[1], Sukrant Sharma[1], Warna Karunasena[1], and Yu Bai[2]

[1]Centre for Future Materials (CFM), School of Civil Engineering and Surveying, Faculty of Health, Engineering and Sciences, University of Southern Queensland, Toowoomba, QLD 4350, Australia

Email: allan.manalo@usq.edu.au; Ging.Maranan@usq.edu.au; u1074865@umail.usq.edu.au; Karu.Karunasena@usq.edu.au

[2]Department of Civil Engineering, Monash University, Clayton, Victoria, Australia

Email: Yu.Bai@monash.edu

Abstract

A comparative study was conducted to evaluate the temperature-sensitive mechanical properties of glass fibre reinforced polymer (GFRP) composites in the longitudinal and transverse directions. GFRP coupons with different shear span-to-depth ratios were tested under three-point static bending test at temperatures ranging from room temperature up to 200^{o}C. Timoshenko Beam Theory-based procedure was then adopted to calculate the flexural and shear moduli of the GFRP laminates under moderate and elevated in-service temperatures. The results showed that the mechanical properties of the transversely cut specimens is affected more by the increase in temperature than the longitudinally cut specimens. Similarly, the interlaminar shear and flexural strengths of GFRP composites were found influenced more by elevated temperature compared to the stiffness properties. Moreover, the shear modulus undergone more severe degradation compared to the flexural modulus. Simplified empirical models were proposed to estimate the mechanical properties of the GFRP pultruded laminates in both the longitudinal and transverse directions at varying temperatures.

Keywords

Interlaminar shear; flexure; elevated temperature; longitudinal direction; transverse direction; comparative study.

*Corresponding author, tel. +61 7 4631 2547; fax. +61 7 4631 2110; E-mail addresses: allan.manalo@usq.edu.au (Allan Manalo)

1. Introduction

Glass fibre reinforced polymer (GFRP) composites have gained wider acceptance as structural materials for civil infrastructure [1, 2] and building construction [3]. This can be attributed to the several advantages of these advanced materials such as lightweight, high strength-to-weight and stiffness-to-weight ratios, corrosion resistance, electromagnetic transparency, ease of handling, and high durability even in harsh environments [4]. Among the GFRPs, the pultruded profiles are the most commonly used because they can be produced in a large volume at low operating costs, high production rate, high fibre content, product reproducibility and dimensional tolerances [2, 5]. However, the sensitivity of the physical and mechanical properties of pultruded GFRP structural profiles to elevated temperatures, due to the glass transition and decomposition processes of the polymer resin, has been one of the major concerns in civil engineering and construction applications. Hence, a better understanding of the resistance behaviours of pultruded GFRP composites under moderate and elevated in-service temperatures must be gained to further advance the adoption and safe use of this material in the mainstream construction applications.

A number of experimental and modelling works have been conducted to characterise the mechanical properties of GFRP composites when exposed to elevated temperatures. Based on these studies, the strength, stiffness and interfacial bonding between the fibres and resin of a pultruded GFRP section decrease as the temperature increases [6-8]. In particular, the aforementioned mechanical properties drop rapidly when the temperature approaches and/or exceeds the glass transition temperature (T_g) of the polymer matrix, typically ranging from 60 ^{o}C to 140 ^{o}C [9]. The elastic modulus of pultruded GFRP composites cut longitudinally (along the direction of pultrusion) is different from those cut transversely; however, dynamic mechanic analysis (DMA) indicated thermal degradation in both directions during the glass transition stage [8]. The degradation of the tensile strength of pultruded GFRP composites at

elevated temperatures is much lower than that of the shear and compressive strengths because the former property is mainly governed by the fibres while the latter properties is dominated by the resin [5]. As a result, various empirical and mechanisms-based models that predict the temperature-dependent properties of composites have been developed, which are generally functions of either mass (or density) and/or temperature [7, 10-14]. Nevertheless, Correia *et al.* [5] stated that additional experimental data are needed to validate previous results and that further research works are needed regarding the other important properties of pultruded composites profiles, particularly the shear modulus, the elastic modulus in the transverse direction and the interlaminar shear strength (ILSS), which is the limiting design characteristic for pultruded FRP [15]. In addition to these properties, the flexural/bending behaviour at elevated temperatures is also of equal importance as input for modelling and design purposes. These aspects are the key motivation of this undertaking.

In this study, the flexural and interlaminar shear behaviour in both the longitudinal and transverse directions of GFRP laminates cut from pultruded sections were comparatively evaluated by subjecting them to temperatures ranging from room temperature (23 °C) to 200 °C. The failure modes, load-deflection curves, load-carrying capacities, and stiffness (linear elastic portion of the load-deflection curves) of these composites were then evaluated. In addition, effects of shear span-to-depth ratio on the longitudinal and transverse properties of the composite laminates were analysed. Thereafter, Timoshenko Beam Theory (TBT)-based procedure [16] was adopted to determine the flexure and shear moduli of the GFRP laminates based on all the experimental results. A simplified empirical models were proposed, calibrated with the test data, to estimate the flexural and shear moduli and strengths of the GFRP pultruded laminates in both the longitudinal and transverse directions at varying temperatures.

2. Experimental Program

2.1 Material

The coupon specimens (Figure 1) considered in this study were prepared from the commercially available GFRP tubular profiles manufactured by Wagner's Composite Fibre Technologies (WCFT) in Toowoomba, Australia. These profiles were made through the pultrusion process, wherein the E-type glass fibre reinforcement are saturated with the catalysed vinyl ester resin and are pulled through the heated curing die to harden and then subsequently cooled. The composite laminates have a stacking sequence in the form [0°/+45°/0°/-45°/0°/-45°/0°/+45°/0°] with a glass fibre content by weight of around 80 % determined in accordance with the ISO 1172:1996 [17] standard. Following the ASTM D792-13 [18], the density was found to be 2050 kg/m^3. The glass transition temperature T_g, on the other hand, was determined through thermomechanical analysis (TMA) using the Model TGA Q500 TA Instrument. Four specimens were preloaded and continuously loaded with 0.02 N and heated at a rate of 10°C/min at temperatures ranging from room temperature (RT), approximately equivalent to 23 °C, up to 180 °C. From the analysis, the average T_g of the laminated composites was 115.6 $^{\circ}$C as shown in Figure 2.

2.2 Specimens

Coupon specimens with average width *b* and thickness *h* of 6.4 mm and 12.1 mm, respectively, but with varying lengths were cut parallel and perpendicular to the pultrusion direction to determine the longitudinal and transverse properties of the pultruded GFRP composites at elevated temperatures. In this study, the mechanical properties, particularly the interlaminar shear and flexural behaviour, of the considered materials were evaluated by testing specimens with shear span-to-depth-ratios *a*/*h* of 4, 8, 15, and 18. Transversely cut specimens with *a*/*h* of 18 were not considered owing to the dimension limitation of the hollow pultruded GFRP square

sections (125 mm by 125 mm by 6.4 mm thickness) to which the coupon specimens were cut from.

The specimens were labelled as Lo-*a*/*h*-*T* and Tr-*a*/*h*-*T* where "Lo" and "Tr" stand for longitudinally and transversely cut specimens, respectively, while *a*/*h* and *T* represent the shear span-to-depth-ratio of the specimen and the temperature in which the specimen was subjected to, respectively. For example, the specimen identified as Lo-4-RT means that it is a specimen cut along the pultrusion direction with an *a/h* of 4 and was tested at room temperature, approximately equivalent to 23°C, while Tr-15-100 means that it is a specimen cut perpendicular to the direction of pultrusion with a *a/h* of 15 and was tested at temperature of 100 °C. Table 1 summarises all the test specimens considered in this study. Five replicates were tested for each test condition for laminates with *a/h* of 4 and 15 while three replicates were tested for other specimen types resulting in a total of 181 test specimens.

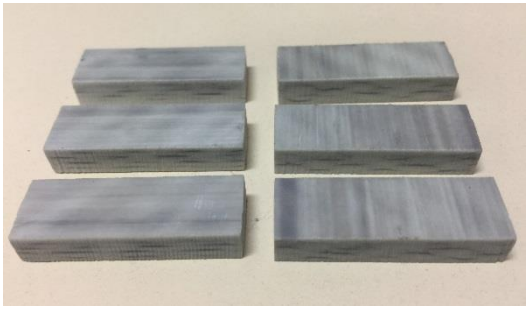

Figure 1. Longitudinally and transversely cut pultruded GFRP coupons

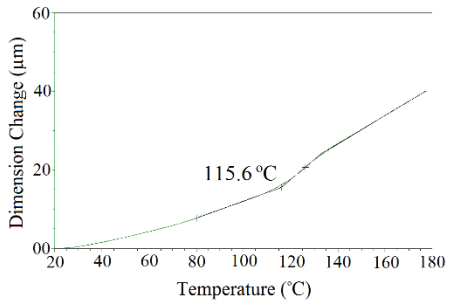

Figure 2. Typical TMA curve of the tested pultruded GFRP laminates composites

Table 1. Summary of the number of test specimens

Orientation	*a*/*h*	Number of Specimens						
		RT	40 °C	70 °C	100 °C	120 °C	150 °C	200 °C
Longitudinal	4	5	5	5	5	--	--	--
	8	3	3	3	3	3	3	--
	15	5	5	5	5	5	5	5
	18	3	3	3	3	3	3	--
Transverse	4	5	5	5	--	--	--	--
	8	5	5	5	5	5	5	5
	15	5	5	5	5	5	5	5

2.3 Test set-up and instrumentation

Figure 3 shows the typical three-point static bending test, following the ASTM D790-15 [19] standard, that was carried out on the pultruded GFRP laminates for two different *a*/*h*. The load was applied at midspan using the 10 kN servo-hydraulic MTS Testing Machine at controlled displacement with a crosshead rate of 1.3 mm/min. During testing, the support span was adjusted at distances (*L*) of 24 mm, 48 mm, 90 mm and 110 mm to achieve the target *a*/*h* values of 4, 8, 15 and 18, respectively.

The specimens were tested at seven different temperatures (RT, 40 ˚C, 70 ˚C, 100 ˚C, 120 ˚C, 150 ˚C and 200 ˚C) using the Instron 3119 environmental chamber. All tests were carried-out under a steady-state condition. After fixing the specimen in the test equipment, the temperature inside the chamber was increased to the target temperature and then held constant for 30 minutes to allow the test specimen to reach the same temperature. In addition to the soaking period in the environmental chamber, the other test specimens were also conditioned inside the chamber while the testing is being conducted. The test specimens were loaded to failure. The peak load, deflection, and failure initiation and progression were monitored and recorded during the tests. After the testing, the failed surfaces of the specimens were examined visually and by using an electron microscope.

(a) *a*/*h* = 4 (b) *a*/*h* = 15

Figure 3. Typical three-point static bending test set-up

3. Results and Observations

*3.1 Behaviour of longitudinally cut specimens (*Lo- *specimens)*

Figure 4 presents the typical load-deflection curves of one representative specimen from all test temperatures. Based on Figures 4a and 4b, Lo-4 and Lo-8 tested at temperatures ranging from RT to 70 °C undergone three stages: the linear stage, the nonlinear stage, and the post-peak stage. The first stage is characterised by a linear elastic segment at lower load that represents the stiffness of the undamaged pultruded GFRP laminates, owing to the elastic behaviour of the matrix and the fibre-matrix interphase during the early stage of loading [20, 21]. The stiffness, however, tend to degrade as the temperature increases. The second stage showed the gradual reduction of stiffness, displayed by a nonlinear curve, which continuously transpired up until the peak load. In the case of Lo-4, the nonlinear behaviour was due to the initiation and propagation of delamination damages, owing to the viscoelastic interlaminar shear behaviour of the resin matrix and the resin-fibre interphase at higher stresses [20, 22], while for Lo-8 that behaviour was caused by the gradual crushing of resin matrix and fibres at the compression zone directly below the point of load application. In general, the nonlinearity increases as the temperature rises. This could be attributed to the glass transition process of the vinylester matrix that caused the initiation and propagation of indentation and furthered the severity of ply delamination (Lo-4) and compression failure (Lo-8) before attaining the peak load. Various post-peak behaviour were observed during the tests. After reaching the ultimate strength, the load-carrying capacity of Lo-4-RT and Lo-4-40 dropped immediately followed by a gradually reducing strength, owing to continuous delamination. Lo-8-RT, on the other hand, yielded a post-peak segment characterised by an abrupt load reduction – due to sudden compression failure – tailed by a slightly increasing load that will drop again, which continuously happened up until the end of load application, owing to the continuous crushing and progressive occurrence of ply delamination. Lo-4-70, Lo-8-40 and Lo-8-70, on the

contrary, exhibited a gradually decreasing capacity due to the combination of indentation, owing to the matrix softening, and progressive crushing and delamination. The remaining Lo-4 and Lo-8 tested at higher temperatures (Lo-4-100, Lo-8-100, Lo-8-120 and Lo-8-150), on the other hand, exhibited a short linear behaviour followed by a more apparent nonlinear behaviour and then tailed by a plastic response due to the transitioning of the resin from a glassy state to a leathery state.

The load-deflection curves of Lo-15 and Lo-18 (Figures 5c and 5d, respectively) tested at temperatures ranging from RT to 70 °C were represented by a two-segment load-deflection curve. The first segment is essentially linear elastic up to the peak load. The second segment or the softening segment, on the other hand, starts with a sharp drop in the load-carrying capacity, due to sudden crushing failure of the fibres and resin matrix. The next segment was due to further compression crushing coupled with the initiation and proliferation of fibre rupture, with some delamination, at the bottom. At 100 °C, the curves of Lo-15 and Lo-18 revealed three different phases (linear, nonlinear, and descending phase) that was similar to that of Lo-4-70 or Lo-8-70. However, the nonlinear and descending phases were governed by fibre and matrix crushing coupled with minor delamination and more apparent indentation due to matrix softening. The rest of Lo-15 and Lo-18 tested at higher temperatures exhibited similar behaviour as Lo-4 and Lo-8 tested from 100 °C to 150 °C.

Figure 5 shows the typical mode of failure of the pultruded GFRP laminates subjected to elevated temperature. As can be expected, all the tested Lo-4 specimens exhibited interlaminar shear failure or ply delamination. Compression crushing directly below the loading point nor fibre rupture at the bottom were neither observed in the tested specimens at room temperature. These observations tends to show the suitability of the employed SBS test in determining the interlaminar shear strength of the pultruded GFRP laminates. At RT and 40 °C, the specimens exhibited a pure ILS failure (Figure 5a) that initiated from several locations

while the specimens tested at 70 °C and 100 °C exhibited a combination of localised delamination and indentation just below the load point due to the softening of the matrix (Figure 5b). Lo-4-70 evidenced more severe delamination compared to Lo-4 tested at lower temperatures. Lo-4-100, in contrast, exhibited more obvious indentation than Lo-4-70 but lesser number of ply delamination compared to Lo-4-RT and Lo-4-40 because the softened resin matrix lost its ability to transfer the stress among the fibres.

The failure of Lo-8 heated from RT to 70 °C was characterised by matrix crushing and fibre fracture, with some kinking, at the top directly below the point of load application coupled with delamination that continuously transpired until the end of the test (Figure 5c), with Lo-8-RT generally failing in a more brittle manner as evidenced by its load-deflection curves and a snapping sound during the tests. Lo-8-40 and Lo-8-70, on the other hand, undergone a ductile failure due to some indentation, which was demonstrated by the gradual strength degradation at the post-peak stage. Generally, the severity of compression crushing and delamination increase with the temperature. Lo-8 specimens tested at 100 °C and 120 °C undergone a more ductile failure owing to the transition of the polymer from glassy state to leathery state. These specimens did not exhibit a compression crushing; however, the failure of these specimens can be described as a concurrent indentation and extensive delamination with fibre kinking between ply boundaries (Figure 5d). Finally, Lo-8-150 undergone a pure delamination since the matrix are already in their leathery state.

Lo-15 and Lo-18 exposed to temperatures between RT to 70 °C, on the other hand, undergone a brittle compression crushing failure of matrix and bending deformation of fibres below the point load followed by the initiation and proliferation of fibre rupture, with minor delamination, at the bottom section (Figure 5e). The degree of compression failure increases with the temperature while the severity of tensile failure decreases because at higher temperature, the resin matrix is more susceptible to compression failure rather than fibre tensile

rupture. At 100 ˚C and 120 ˚C, Lo-15 and Lo-18 failed in a ductile manner, which can be described as fibre kinking and buckling, because the softened resin can no longer confine the glass fibres, coupled with resin crushing at the top directly below the point load but without any fibre rupture (Figure 5f). These observations can be expected since the softened resin matrix at the compression zone have a lower capability to prevent damages compared to the temperature-resistant E-glass fibres and flexible matrix at the tensile zone. With further loading, the damages accumulate gradually in the specimens tested at higher temperatures, as reflected in their load-deflection curves. The remaining specimens subjected to temperature 150 ˚C and 200 ˚C undergone delamination that originated at the free end and then propagated towards the midspan of the specimens (Figure 5g).

3.2 Behaviour of transversely cut specimens (Tr- specimens)

Tr-4, Tr-8 and Tr-15 tested from RT to 200 °C also yielded a three-segment load-deflection curves (Figures 4e, 4f and 4g, respectively). The first segment represents the linear elastic behaviour at lower applied loads, which embodies the stiffness of the pultruded GFRP laminates in the transverse direction. With further loading, a nonlinear behaviour occurred, wherein the stiffness decreased gradually prior to peak load, which corresponds to the second segment of the curve. At this stage, several abrupt load drops happened in specimens tested at RT due to the progressive formation of flexural cracks, with some crack-induced delamination, at the bottom section. As the temperature rises, the linear portion of the curve shortened while the nonlinear segment increases, owing to the softening of the vinylester matrix. After reaching the maximum load, the load-carrying capacity of Tr- specimens tested at RT dropped rapidly while those subjected to temperatures ranging from 40 °C to 100 °C yielded a gradually decreasing capacity. The remaining Tr- specimens exposed at 120-200 °C, however, yielded a plateau segment that represents the plastic behaviour of the polymer in its leathery material state.

All Tr- specimens undergone a failure characterised by the formation of vertical and inclined cracks at the bottom section of the laminates, followed by some crack-induced delamination, which is considered as a flexure-type of failure. The development of bottom flexural cracks in transversely cut specimens seems to be concentrated and/or localised in one location, approximately at the midpsan of the specimen, when tested at room temperature (Figure 5h). The crack widened and propagated upward as the applied load increases. At higher temperature, however, the cracks were randomly distributed at the bottom of the specimens (Figure 5i). As the temperature increases, the number of cracks and frequency of crack-induced delamination increase while the crack width becomes narrower.

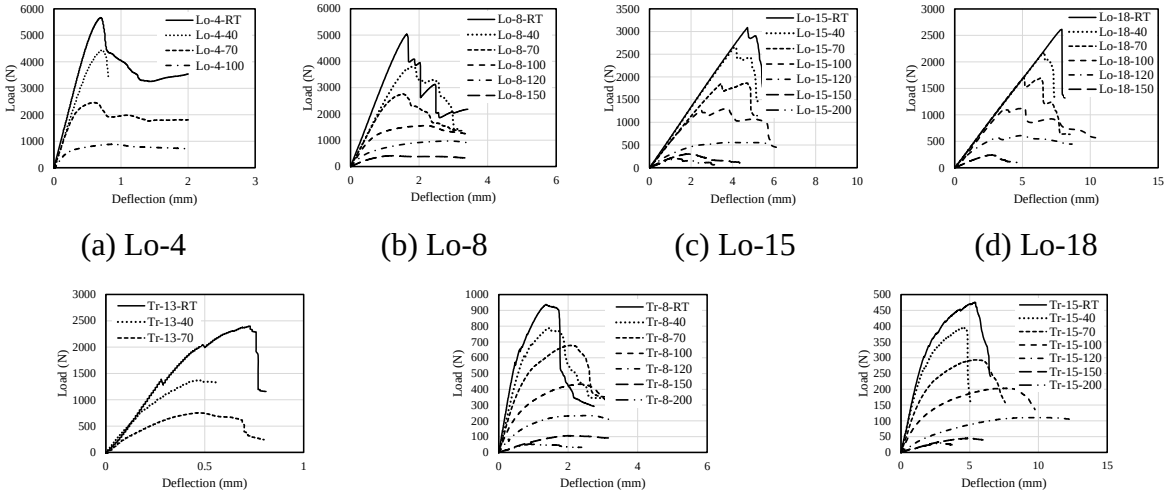

(a) Lo-4 (b) Lo-8 (c) Lo-15 (d) Lo-18

(e) Tr-4 (f) Tr-8 (g) Tr-15

Figure 4. Typical load-deflection curves of GFRP laminates at moderate and elevated temperatures

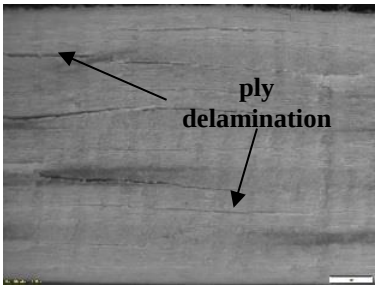

(a) delamination (Lo-4-23 and Lo-4-40)

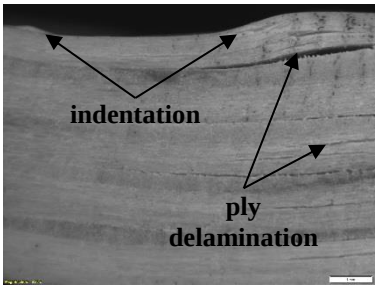

(b) delamination with indentation (Lo-4-70 and Lo-4-100)

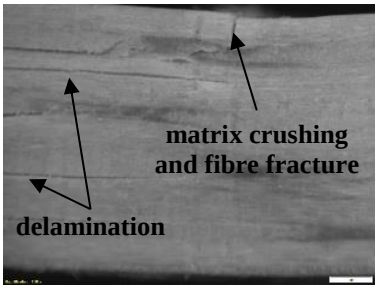

(c) matrix crushing and fibre fracture followed by some delamination (Lo-8-RT to Lo-8-70)

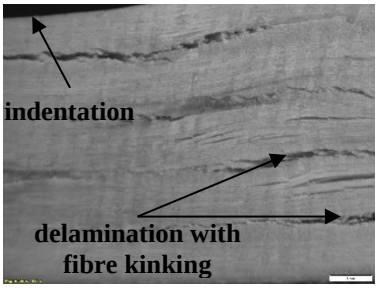

(d) indentation and delamination with fibre kinking (Lo-8-100 to Lo-8-150)

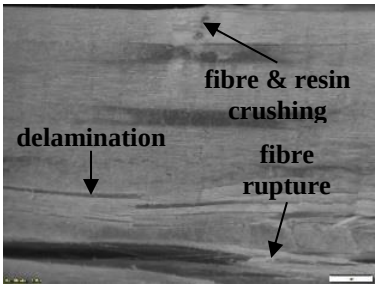

(e) fibre and resin crushing at the top followed by delamination and fibre rupture at the bottom (Lo-15 and Lo-18 tested between RT and 70 °C)

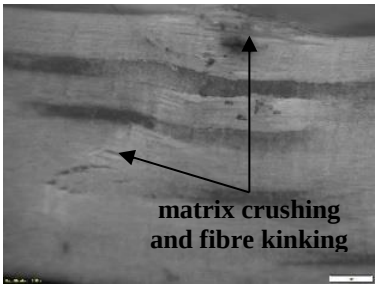

(f) matrix crushing and fibre kinking (Lo-15 and Lo-18 tested between 100 °C and 120 °C)

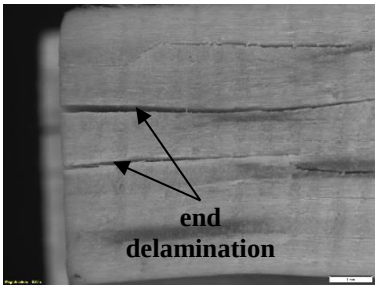

(g) delamination at the free end of the specimens (Lo-15 and Lo-18 tested between 150 °C and 200 °C)

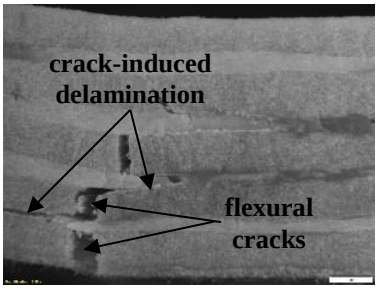

(h) localised flexural cracks with crack-induced delamination (all Tr- specimens tested at RT)

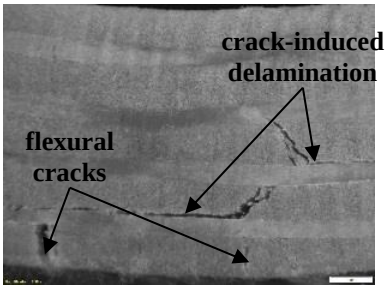

(i) distributed flexural cracks with crack-induced delamination (all Tr- specimens tested at 40-200 °C)

Figure 5. Typical failure modes of pultruded GFRP laminates at elevated temperatures

4. Discussion

4.1 Interlaminar shear strength

Table 2 summarises the average peak load capacity *P* and the corresponding average interlaminar shear strength *ILSS* of specimens with *a*/*h* of 4. Figure 6a, on the other hand, illustrates the normalised *ILSS* of the specimens, with respect to their values at room temperature, as a function of temperature. The *ILSS* is calculated using the equation below.

$$ILSS = \frac{3 \times P}{4 \times w \times h} \qquad \text{Equation 1}$$

Based on the table and figure, the *ILSS* of longitudinally cut GFRP laminates at room temperature is around 54.7 MPa. This value was comparable to that reported by Muttashar *et al.* [23], equivalent to 51 MPa, for the same pultruded GFRP section. In general, the strength of Lo-4 tend to decline steadily, at a constant gradient, as the temperature rises. Interestingly, this linear trend was also observed by Liu *et al.* [20] for carbon fibre-reinforced epoxy resin composites tested from ambient temperature to 130 °C. It can be inferred that this strength degradation at higher temperatures was due to the softening of the resin matrix that resulted in the reduction of the shear stress resistance and the occurrence of indentation failure. In fact, at 100°C, the load-carrying capacity retention of Lo-4 was just 14%. At this temperature exposure, the resin drastically losses its ability to hold the fibres together, including the ability to transfer interfacial shear stress from one portion to another, as evidenced by the localised ply delamination (in the vicinity of point load application) in these specimens. Beyond 100°C, the specimens did not sustain further loads, suggesting that the tested vinylester-based GFRP laminates have negligible *ILSS* when exposed to temperature just below the T_g of the resin matrix.

The strength of Tr-4 was also negatively affected by the elevated temperature exposure as can be noted from Table 2 and Figure 6a. These specimens yielded a negligible strength at 70°C. At higher temperature, several flexural cracks were formed at different locations, instead

of one single major cracks, that lowered the strength capacity of the specimens. The maximum capacity attained by Tr-4 specimens at room temperature was only approximately 40% of Lo-4's ultimate strength. This can be expected since the strength of Lo- specimens was enhanced by the longitudinally oriented (0°) fibres. Furthermore, the strength degradation of Tr- specimens was more severe compared to Lo- specimens as the temperature increases. Again, this is because Tr- specimens have no 0° fibres that can support the softened matrix in resisting applied loads that resulted in a relatively more strength loss.

4.2 Flexural strength

Table 3 shows the mean peak strength P and the corresponding average maximum bending strength σ of the flexural specimens with a/h of 8, 15 and 18, tested at varying temperatures while Figure 6b, 6c and 6d plot the flexural strength of the pultruded GFRP laminates as a function of temperature normalised to that measured at room temperature. The flexural strength was calculated from Equation 2.

$$\sigma = \frac{3 \times P \times L}{2 \times w \times h^2} \qquad \text{Equation 2}$$

As shown in Table 3, Lo-15 and Lo-18 yielded load-carrying capacities of 3014 N and 2405 N, respectively, at room temperature. These loads were equivalent to σ of 821 MPa and 801 MPa, respectively, which were almost the same with the results obtained by Guades *et al*. [24] for the same materials. Interestingly, the measured strength was more than twice the strength (325 MPa) reported by Liao *et al.* [25] for glass fibre-vinyl ester composite. This could be attributed to the type and configuration of the fibres they adopted in their study, consisting of alternating layers of unidirectional fibre roving and chopped fibre strand mat, including the fibre-matrix interphase properties.

The load-carrying capacities of Lo-8, Lo-15 and Lo-18 tested at temperatures 23-100°C tend to decrease linearly but with different level of strength degradation, with Lo-8 exhibiting more steep strength decay compared to the other specimens. As the temperature increases,

softening and cracking in the compression zone progressively transpired that reduced the mechanical properties of the resin, including the resin-fibre bond, making the composite to progressively act like a bundle of loose fibres instead of a solid composite. The decrease of bond efficiency impairs the stress transfer within the composites, thereby lowering the overall load resistance of the material. Substantial strength reduction occurred when the specimens were tested at temperature 120 °C. This can be expected since this exposure temperature exceeded the measured T_g (115.6 °C) of the vinylester matrix. During this stage, the softened vinylester matrix losses the ability to resist compression stresses and to transfer stresses amongst fibres, including the ability to bind and hold the fibres together to prevent fibre buckling in the compression zone [26, 27], as evidenced by the severe compression failure of the tested specimens. At 120 °C, the residual strengths were just 20%, 19%, and 22%, respectively, of their corresponding strengths at room temperature. The strength continued to decline at temperature 150 °C, but this time, the degree of reduction from 120 °C to 150 °C was relatively lower compared to the declination from 100 °C to 120 °C, and even became lesser from 150 °C to 200 °C. Tr-8 and Tr-15, on the other hand, yielded an almost similar load-carrying capacity pattern characterised by a steady strength degradation starting from room temperature up until 120 °C, owing to similar mode of failure (flexural cracking at the bottom) of these specimens even at higher temperatures. From single major crack at low temperature, the specimens evidenced several flexural cracks at the bottom at higher temperature. The strength retention of Tr-8 and Tr-15 at 120 °C was approximately 26%. The strength reduction, however, tends to stabilise at 150-200 °C.

The flexural strength increases when *a/h* decreases because the portion of the point loads that are directly being transferred to the support – through a strut – increases, i.e., the composite laminate's behaviour was dominated by the arch action instead of the beam action when *a/h* decreases. Lo-15 and Lo-18's average strength at ambient temperature were 62 %

and 103 %, respectively, lower than Lo-8 while Tr-15 produced an average strength that was 110 % lesser than Tr-8. In general, the longitudinally cut specimens yielded higher strength compared to transversely cut specimens for similar temperature exposure. At room temperature, the strength of Lo-8 and Lo-15 were 416 % and 570 %, respectively, greater than that of Tr-8 and Tr-15, respectively. The degree of strength reduction per defined temperature rise, however, was larger in the former specimens compared to the latter samples. This is because at low temperature, the stresses are effectively transferred from fibres to resin matrix and vice versa; however, at higher temperature, the matrix loss its ability to transfer stresses that resulted in higher strength degradation. The transversely cut specimens, on the other hand, was mainly governed by the matrix all throughout the test and hence, a steep strength reduction was observed as the temperature rises.

4.3 Stiffness

Based on Table 2 and Figure 6a, the stiffness – the slope of the linear elastic portion of the load-deflection curves P/Δ – of Lo-4 was 87 % higher than that of Tr-4 at room temperature. In addition, Lo-4 exhibited an excessive stiffness degradation at temperatures between 70 °C and 100 °C while Tr-4 undergone same phenomenon when tested between 40 °C and 70 °C, suggesting that the stiffness of transversely cut specimens seems to be more influenced by the temperature compared to longitudinally cut specimens. This is because of the ability of Lo-4 specimens to transfer the applied load from matrix to 0° and $\pm$ 45^{o} fibres and vice versa compared to Tr-4.

In general, all the samples exhibited stiffness degradation with increased temperature as shown in Table 3 and Figures 6b, 6c and 6d. Lo-8, Lo-15, Lo-18, Tr-8 and Tr-15 undergone an almost linear stiffness reduction from room temperature up until 100 °C. However, a significant modulus drop occurred between 100 °C and 120 °C. At 120 °C, the stiffness of Lo-8, Lo-15 and Lo-18 were 37 %, 51 %, and 57 %, respectively, of their stiffness at room

temperature while that of Tr-8 and Tr-15 were just 23 % and 25 %, respectively. On the other note, the measured flexural modulus was more than two times greater than that of Liao *et al.*'s [25] tested glass fibre-vinyl ester composites. Similar with the strength property, an inverse relationship was observed between the stiffness and *a/h*. At room temperature, Lo-8's mean stiffness was 405 % and 819 % higher than that of Lo-15 and Lo-18, respectively, while that of Tr-8 was 486 % more than Tr-15's stiffness. On a different note, Lo-8 and Lo-15 yielded stiffness that were 2.8 and 3.2 times, respectively, bigger than that of Tr-8 and Tr-29. Furthermore, as the temperature increases, stiffness degradation was relatively more severe in Tr- specimens compared to Lo- specimens.

It was apparent from Figure 6 that for similar elevated temperature exposure, the load-carrying capacity of the longitudinally cut specimens undergone higher degree of degradation compared to their stiffness, suggesting that the strength of the longitudinally cut pultruded GFRP laminates was more influenced by the temperature compared to its stiffness. This is because the former mechanical property was mainly governed by the resin properties and the corresponding fibre-matrix interaction while the latter property was predominantly influenced by the fibre properties [28, 29]. Interestingly, this observation corroborates with that of Correia *et al.* [9] who conducted an in-plane shear strength tests, through 10° off-axis tensile tests, on GFRP composites. From their experiment, they concluded that the relative reduction of shear strength was significantly larger than that of shear stiffness due to glass fibres that retain considerable amount of room temperature stiffness. Another reason is that the distribution of stresses among the glass fibres (in both the compression and tension zones) at higher temperature became less uniform because the softened resin can no longer confine and hold the glass fibres inside the matrix, which leads to substantial reduction of the load-carrying capacity.

Tr-8 and Tr-15 specimens yielded almost similar degree of strength and stiffness degradation, mainly because the mechanical transverse properties are predominantly governed by the resin matrix. This result tend to support Lahuerta et al.'s [30] hypothesis wherein they stated that the transverse strength and moduli are related to resin properties. However, this was not the case for Tr-4 specimens, the strength falls more sharply than the slope of the load-deflection curve. This is due to the interlaminar shear strength in the transverse direction is affected more by the weakening of the interface between the fibres and the matrix while the $\pm 45^{o}$ fibres are still contributing to the shear modulus of the laminates.

The average stiffness at room temperature of Lo-15 and Lo-18 were approximately equivalent to 647 N/mm and 355 N/mm, respectively, which translate to flexural moduli *E* of 37.2 GPa and 37.3 GPa, respectively, wherein *E* was computed from Equation 3. The computed flexural moduli were generally comparable to the published flexural moduli of 36.1 GPa [24] and 39.3 MPa [23] for the same pultruded GFRP coupons.

$$E = \frac{(P/\Delta) \times L^3}{4 \times w \times h^3} \qquad \text{Equation 3}$$

Table 2. Average peak load capacity *P*, interlaminar shear strength *ILSS*, and stiffness *P*/Δ of the specimens with *a*/*h* of 4 at elevated temperatures.

Specimen	*P*, N	*ILSS*, MPa	*P*/Δ, N/mm	Specimen	*P*, N	*ILSS*, MPa	*P*/Δ, N/mm
Lo-4-RT	5643 (194)	55 (2)	9799 (366)	Tr-4-RT	2147 (198)	21 (2)	5234 (103)
Lo-4-40	4183 (183)	41 (2)	8188 (644)	Tr-4-40	1323 (42)	13 (1)	4743 (314)
Lo-4-70	2449 (124)	24 (1)	7783 (333)	Tr-4-70	5 (1)	0 (0)	2519 (449)
Lo-4-100	810 (62)	8 (1)	3877 (220)				

Note: The numbers inside ( ) are the standard deviations.

Table 3. Average peak load capacity P, flexural strength σ, and stiffness P/Δ of the specimens with a/h of 8, 15 and 18 at elevated temperatures.

Specimen	P, N	σ, MPa	P/Δ, N/mm	Specimen	P, N	σ, MPa	P/Δ, N/mm
Lo-8-RT	4873(243)	708 (35)	3267 (153)	Tr-8-RT	945 (11)	137 (2)	1172 (51)
Lo-8-40	3742 (71)	544 (10)	2645 (4)	Tr-8-40	791 (21)	115 (3)	1015 (73)
Lo-8-70	2847 (117)	414 (17)	2583 (92)	Tr-8-70	671 (12)	98 (2)	787 (51)
Lo-8-100	1558 (5)	226 (1)	2055 (22)	Tr-8-100	442 (29)	64 (4)	525 (54)
Lo-8-120	965 (8)	140 (1)	1220 (23)	Tr-8-120	257 (34)	37 (5)	265 (75)
Lo-8-150	388 (29)	56 (4)	554 (14)	Tr-8-150	99 (13)	14 (2)	70 (6)
				Tr-8-200	51 (5)	7 (1)	64 (6)
Lo-15-RT	3014 (12)	821 (33)	647 (24)	Tr-15-RT	450 (28)	123 (8)	200 (19)
Lo-15-40	2636 (15)	718 (41)	620 (37)	Tr-15-40	367 (43)	100 (12)	185 (13)
Lo-15-70	1805 (10)	492 (28)	558 (57)	Tr-15-70	309 (17)	84 (5)	148 (11)
Lo-15-100	1269 (60)	346 (16)	547 (12)	Tr-15-100	195 (25)	53 (7)	115 (13)
Lo-15-120	568 (33)	155 (9)	327 (25)	Tr-15-120	112 (3)	31 (1)	49 (8)
Lo-15-150	298 (18)	81 (5)	191 (29)	Tr-15-150	43 (4)	12 (1)	13 (1)
Lo-15-200	181 (27)	49 (7)	185 (30)	Tr-15-200	25 (3)	7 (1)	11 (1)
Lo-18-RT	2405 (29)	801 (9)	355 (16)	Lo-18-100	1098 (53)	365 (18)	304 (4)
Lo-18-40	2231 (59)	743 (20)	337 (32)	Lo-18-120	536 (14)	178 (38)	202 (45)
Lo-18-70	1664 (52)	554 (17)	331 (20)	Lo-18-150	236 (8)	78 (3)	111 (1)

Note: The numbers inside ( ) are the standard deviations.

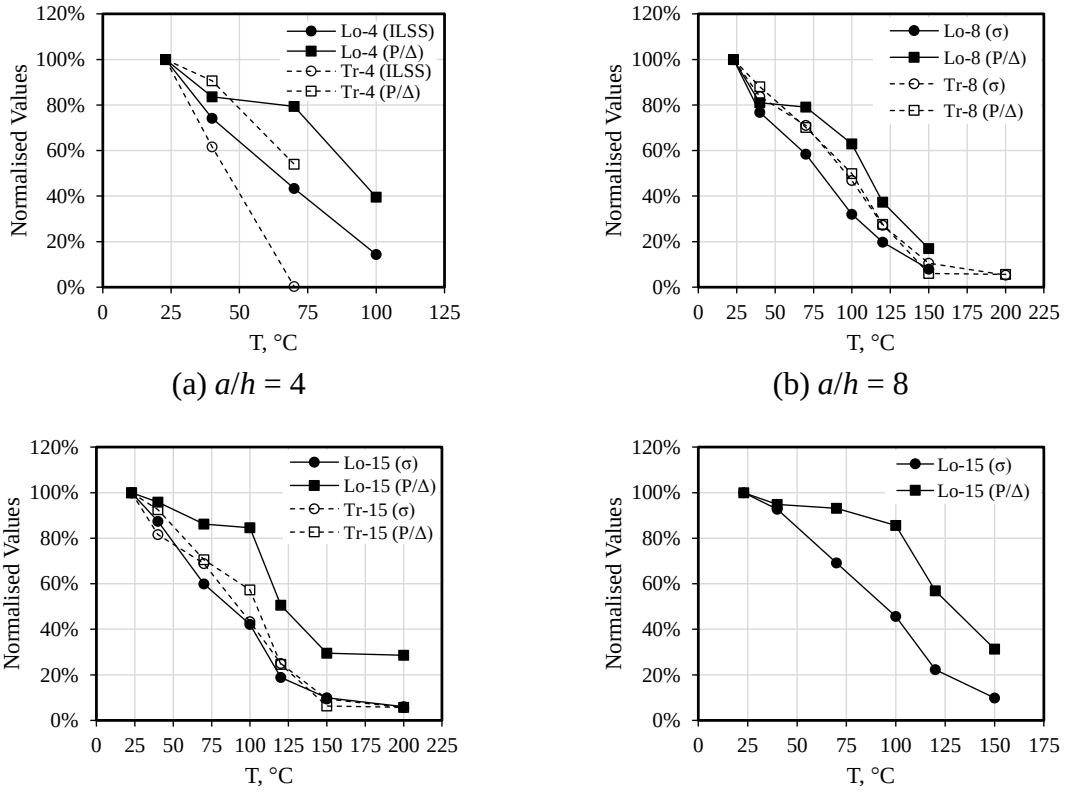

(a) a/h = 4 (b) a/h = 8

(c) a/h = 15 (d) a/h = 18

Figure 6. Normalised strength and stiffness as a function of temperature

4.4 Flexural and Shear Moduli based on Timoshenko Beam Theory

The low shear modulus of the resin compared to the elastic modulus of the fibres resulted in a relatively low shear-modulus-to-elastic-modulus ratio of the composites that made the shear deformation very significant in the overall deformation and hence, must be considered in the calculation of the total deflection [31, 32]. Therefore, the Timoshenko Beam Theory (TBT)-based procedure [16] was adopted in this study to determine simultaneously the flexural and shear moduli of the pultruded GFRP composite laminates using the experimental results. According to this theory, the total maximum deflection (Δ) can be computed as the sum of the deflections due to flexural and shear deformations (Δ_f and Δ_s, respectively). For composite beams tested under three-point bending test, the equation is written as follows:

$$\Delta = \Delta_f + \Delta_s = \frac{PL^3}{48EI} + \frac{PL}{4KGA} \qquad \text{Equation 4}$$

where P is the vertical load applied at midspan; L is the clear span or distance between the supports; E and G are the flexural and shear moduli; I and A are the centroidal moment of inertia and cross-sectional area, respectively; and K is the shear area coefficient (assumed as 1.0 in this study). In order to determine E and G, Equation 4 can be written as follows:

$$\frac{4A\Delta}{PL} = \frac{1}{12E}\left(\frac{L}{r}\right)^2 + \frac{1}{G} \qquad \text{Equation 5}$$

This equation can be interpreted as a straight line with quantities $4A\Delta/PL$ and $(L/r)^2$ as the dependent and independent variables, respectively, while $1/12E$ and $1/G$ as the slope (m) and y-ordinate (c), respectively. Hence, E and G can be computed as follows:

$$E = \frac{1}{12m} \qquad \text{Equation 6}$$

$$G = \frac{1}{c} \qquad \text{Equation 7}$$

Following Equation 5, new graphs $4A\Delta/PL$ versus $(L/r)^2$ were plotted for each series of longitudinally and transversely cut specimens as shown in Figures 7 and 8, respectively. A linear regression was conducted in order to determine m and b, which are shown in the figures.

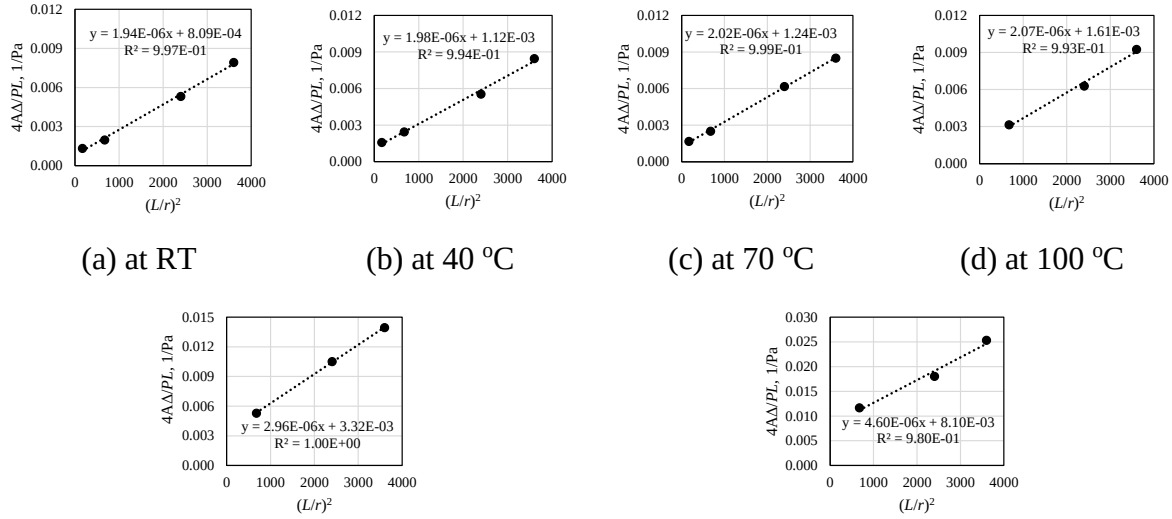

(a) at RT (b) at 40 ºC (c) at 70 ºC (d) at 100 ºC

(e) at 120 ºC (f) at 150 ºC

Figure 7. $4A\Delta/PL$ and $(L/r)^2$ of Lo- specimens at elevated temperatures

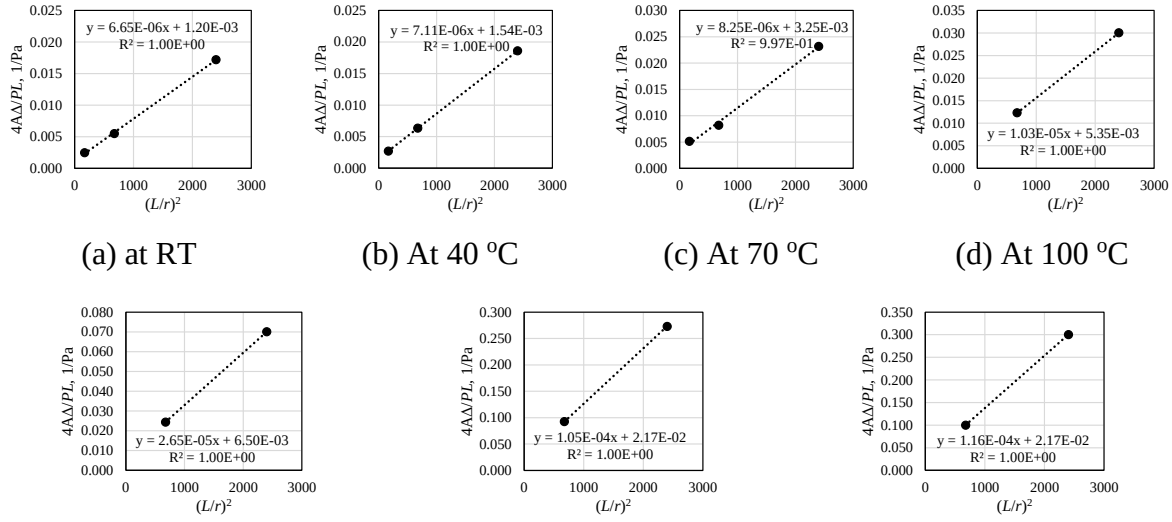

(a) at RT (b) At 40 ºC (c) At 70 ºC (d) At 100 ºC

(e) At 120 ºC (f) At 150 ºC (g) Tr-15

Figure 8. $4A\Delta/PL$ and $(L/r)^2$ of Tr- specimens at elevated temperatures

Table 4 summarises the values of E and G of the longitudinally and transversely cut specimens derived from TBT using Equations 6 and 7. The flexural modulus of Lo- specimens at room

temperature (42.9 GPa) was larger than that obtained from either Lo-15 (37.2 GPa) and Lo-18 (37.3 GPa). This can be expected since the total deflection (deflection due to bending as well as shear deformations), instead of the deflection due to flexural deformations only, was used to calculate *E* of Lo-15 and Lo-18. The longitudinal shear modulus at room temperature, on the other hand, was approximately equal to 1.2 GPa. It is important to note that this value was just 22% of the in-plane shear modulus reported by Muttashar *et al*. [23].

The elastic and shear moduli decrease as the temperature increases, wherein a drastic moduli degradation occurred when the temperature exposure exceeded the T_g of the vinylester matrix, specifically at 120 °C. Again, this was due to the transitioning of the resin matrix from a rigid glassy state to a flexible leathery state, as explained in the previous sections. Interestingly, for similar temperature exposure, the degree of flexural moduli degradation based on TBT theory was relatively similar to that Lo-15 and Lo-18, suggesting the suitability of Bank's proposed procedure in determining not only the *E* values but also the *G* values of the GFRP laminates at elevated temperatures. By inspecting Table 4, as the temperature increases, the shear modulus property exhibited more steep degradation compared to flexural modulus because the former is mainly dependent on the resin properties, which are significantly reduced at higher temperature.

The moduli of the longitudinally cut specimens were generally higher than those cut transversely. At RT, Lo- specimens' *E* and *G* were 223 % and 48 %, respectively, higher than that of Tr- specimens. At higher temperatures, the difference even became higher. In fact, for similar temperature exposure, the flexural and shear moduli of transversely cut specimens decreased more drastically in comparison with the longitudinally cut specimens. This observation tend to suggest that the influence of +45° and -45° fibres to the mechanical properties in the transverse direction tend to decrease at higher temperatures. This behaviour was different from that reported by Bai *et al.* [8] regarding the DMA tests conducted on

pultruded GFRP laminates cut along the two directions wherein they reported that although different in magnitude, the moduli in the longitudinal and transverse direction undergone similar trend at elevated temperatures. This could attributed to the fibre composition and orientation they adopted in their study which is a combination of a chopped strand mat (CSM) and a woven roving [0°/90°] that resulted to similar properties in both direction.

Table 4. Summary of *E* and *G* values based on TBT-theory

Temperature (°C)	Lo- specimens		Tr- specimens	
	E, MPa	*G*, GPa	*E*, MPa	*G*, GPa
RT	42.9	1.2	12.5	0.8
40	42.1	0.9	11.7	0.6
70	41.2	0.8	10.1	0.3
100	40.2	0.6	8.1	0.2
120	28.1	0.3	3.1	0.1
150	18.1	0.1	0.8	0.0
200	-	-	0.7	0.0

5. Prediction Equation of Strength and Stiffness

Simplified prediction equations that can accurately model the variation of the mechanical properties at different temperature exposure are necessary in the of design structures with FRP components [7]. Figure 9 plots the flexural and shear moduli as a function of temperature. Based on the figure, the *E*- modulus of both the longitudinally and transversely cut specimens decrease linearly from room temperature up until 100 °C. Then, from 100 °C to 150 °C, the flexural modulus exhibited more steep linear degradation. The *G*- modulus, on the contrary, tends to reduce linearly from room temperature up to 150 °C.

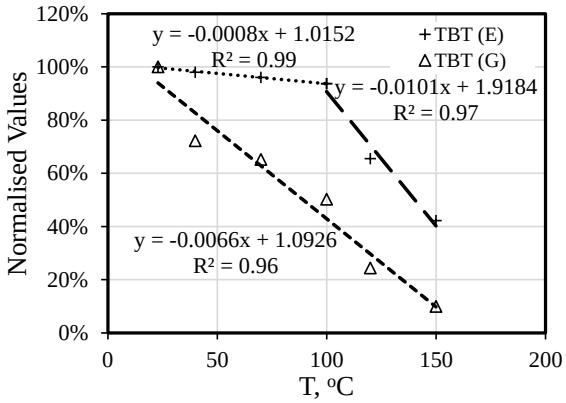

(a) Lo- specimens

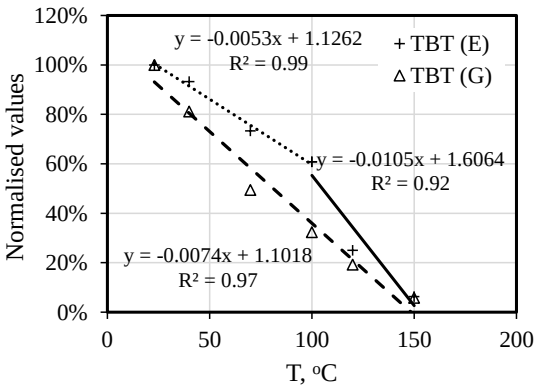

(b) Tr- specimens

Figure 10. Flexural and shear moduli as function of temperature

Based on these observations, regression analyses were done to determine the appropriate empirical models that will best describe the moduli of the GFRP laminates and their corresponding deflection when subjected to moderate and elevated temperatures. From the analyses, the following equations were proposed for the studied GFRP laminates:

Along the pultrusion direction:

$$\Delta_{Lo} = \frac{PL^3}{48E_{Lo}I} + \frac{PL}{4G_{Lo}A} \qquad \text{Equation 8}$$

$$E_{Lo} = E_{Lo-RT}\left(-0.0008T + 1.0152\right) \text{when RT} \leq T \leq 100\ ^{o}\text{C} \qquad \text{Equation 8-1}$$

$$E_{Lo} = E_{Lo-RT}\left(-0.0101T + 1.9184\right) \text{when } 100\ ^{o}\text{C} < T \leq 150\ ^{o}\text{C} \qquad \text{Equation 8-2}$$

$$G_{Lo} = G_{Lo-RT}\left(-0.0066T + 1.0926\right) \text{when RT} \leq T \leq 150\ ^{o}\text{C} \qquad \text{Equation 8-3}$$

where E_{Lo} and G_{Lo} are the flexural and shear moduli along the direction of pultrusion that are functions of the longitudinal flexural and shear moduli at room temperature ($E_{Lo\text{-}RT}$ and $G_{Lo\text{-}RT}$, respectively) and temperature T.

Perpendicular to the pultrusion direction:

$$\Delta_{Tr} = \frac{PL^3}{48E_{Tr}I} + \frac{PL}{4G_{Tr}A} \qquad \text{Equation 9}$$

$$E_{Tr} = E_{Tr-RT}\left(-0.0053T + 1.1262\right) \text{ when RT} \leq T \leq 100\ ^{o}\text{C} \qquad \text{Equation 9-1}$$

$$E_{Tr} = E_{Tr-RT}\left(-0.0105T + 1.6064\right) \text{ when } 100\ ^{o}\text{C} < T \leq 150\ ^{o}\text{C} \qquad \text{Equation 9-2}$$

$$G_{Tr} = G_{Tr-RT}\left(-0.0074T + 1.1018\right) \text{ when RT} \leq T \leq 150\ ^{o}\text{C} \qquad \text{Equation 9-3}$$

where E_{Tr} and G_{Tr} are the flexural and shear moduli perpendicular to the direction of pultrusion that are functions of the transverse flexural and shear moduli at room temperature ($E_{Tr\text{-}RT}$ and $G_{Tr\text{-}RT}$, respectively) and temperature T.

Figure 10 shows the variation of the interlaminar shear strength and flexural strength of the composite laminates with the temperature. From the figure, the *ILSS* and flexural strength of both the longitudinally and transversely cut specimens decrease linearly at temperatures ranging from ambient temperature (23 °C) up to 150 °C. From this observation, the following prediction equations that can estimate the *ILSS* and flexural strength of the tested GFRP composite laminates at in-service elevated temperatures were proposed:

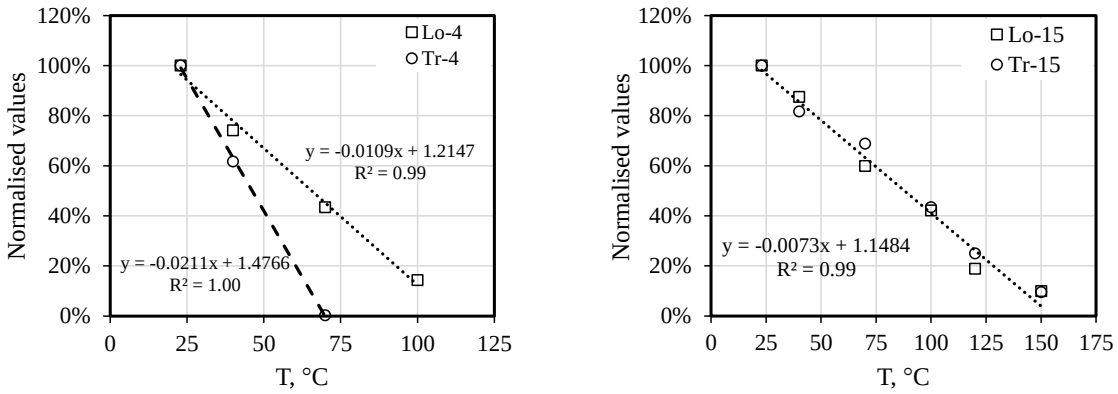

(a) ILSS (b) Flexural strength

Figure 10. ILSS and flexural strength as function of temperature

Along the pultrusion direction:

$$ILSS_{Lo} = ILSS_{Lo-RT}\left(-0.0211T + 1.4766\right) \text{ when RT} \leq T \leq 100\ ^{o}\text{C} \qquad \text{Equation 10}$$

$$\sigma_{Lo} = \sigma_{Lo-RT}\left(-0.0073T + 1.1484\right) \text{ when RT} \leq T \leq 150\ ^{o}\text{C} \qquad \text{Equation 11}$$

Perpendicular to the pultrusion direction:

$$ILSS_{Tr} = ILSS_{Tr-RT}\left(-0.0109T + 1.2147\right) \text{ when RT} \leq T \leq 70\ ^{o}\text{C} \qquad \text{Equation 12}$$

$$\sigma_{Tr} = \sigma_{Tr-RT}\left(-0.0073T + 1.1484\right) \text{ when RT} \leq T \leq 100\ ^{o}\text{C} \qquad \text{Equation 13}$$

where $ILSS_{Lo\text{-}RT}$ and $\sigma_{Lo\text{-}RT}$ are the longitudinal interlaminar shear strength and flexural strength at room temperature, respectively, while $ILSS_{Tr\text{-}RT}$ and $\sigma_{Tr\text{-}RT}$ are the transverse interlaminar shear strength and flexural strength at room temperature, respectively.

6. Conclusions

In this study, longitudinally and transversely cut pultruded GFRP composite laminates were considered and tested using the three-point bending test to investigate its mechanical properties when subjected to elevated temperatures. Based on the test, the following conclusions were derived:

- In general, the strength and stiffness of the tested composite laminates decreased when the temperature increases, with significant reductions occurring between 100°C to 150°C due to the glass transition process undergone by the matrix (vinylester resin).
- For the same degree of temperature exposure, the interlaminar shear strength *ILSS*, shear modulus, flexural strength, and elastic modulus of transversely cut specimens undergone more severe degradation compared to that of longitudinally cut specimens. This could be attributed to the presence of more fibres, oriented along the pultrusion direction, resisting the applied load which made the longitudinal mechanical properties of the GFRP composite laminates better than its transverse properties.

- As the shear-span-to-depth-ratio *a*/*h* decreases, the strength degradation at elevated temperature became more drastic in both longitudinal and transverse directions. In fact, the specimens with *a*/*h* of 4 were able to carry interlaminar shear stress up to temperature exposure of 70°C only while those with *a*/*h* of 15 and 18 were able to sustain flexural stresses until 200°C. This is because the stress resistance mechanism of the former specimens was generally governed by the fibre-resin interphase properties, which is directly affected by the degradation of polymer resin at elevated temperature, while that of the latter specimens were predominantly coming from the compressive strength of the resin and glass fibres and the tensile strength of the fibres.
- At elevated temperature, the shear modulus undergone more severe degradation compared to flexural modulus because the shear modulus of the pultruded GFRP laminates is mainly dependent on the interaction between the fibre and matrix while the flexural modulus is predominantly influenced by the fibre properties.
- The strength of the longitudinally cut specimens was more influenced by the elevated temperature compared to its stiffness, mainly because the strength was governed by the fibre-matrix interaction while the stiffness was affected by the fibre properties. On the contrary, the strength and stiffness behaviour of transversely cut specimens, undergone similar trend of degradation in strength and stiffness as both these properties are predominantly dependent on the resin matrix.
- Simplified empirical models to predict the strength and modulus of the GFRP laminates in both the longitudinal and transverse directions at elevated temperature were proposed. Further experimental works, however, are needed to enhance the accuracy of these equations.

The knowledge and gained from this study would be substantial in the development of design curves that simulate the degradation of the temperature-dependent mechanical performance,

which would be useful in analysing the response of the pultruded GFRP structural profiles and of various assemblies built out of it under elevated temperature.

Nomenclature:

a = shear span (mm)

A = cross-sectional area of the laminate (mm^2)

b = width of the laminate (mm)

c = y-ordinate of the line

E = flexural modulus (MPa, GPa)

E_{Lo} = flexural modulus along the pultrusion direction (MPa, GPa)

$E_{Lo\text{-}RT}$ = flexural modulus along the pultrusion direction at room temperature (MPa, GPa)

E_{Tr} = flexural modulus perpendicular to the pultrusion direction (MPa, GPa)

$E_{Tr\text{-}RT}$ = flexural modulus perpendicular to the pultrusion direction at room temperature (MPa, GPa)

G = shear modulus (MPa, GPa)

G_{Lo} = shear modulus along the pultrusion direction (MPa, GPa)

$G_{Lo\text{-}RT}$ = shear modulus along the pultrusion direction at room temperature (MPa, GPa)

G_{Tr} = shear modulus perpendicular to the pultrusion direction (MPa, GPa)

G_{Tr} = shear modulus perpendicular to the pultrusion direction at room temperature (MPa, GPa)

h = thickness of the laminate (mm)

I = centroidal moment of inertia of the laminate (mm^4)

$ILSS$ = interlaminar shear strength (MPa)

$ILSS_{Lo}$ = interlaminar shear strength along the pultrusion direction (MPa)

$ILSS_{Lo-RT}$ = interlaminar shear strength along the pultrusion direction at room temperature (MPa)

$ILSS_{Tr}$ = interlaminar shear strength perpendicular to the pultrusion direction (MPa)

$ILSS_{Tr-RT}$ = interlaminar shear strength perpendicular to the pultrusion direction at room temperature (MPa)

K = shear are coefficient (assumed as 1.0 in this study)

L = span, clear distance between supports (mm)

L/r = slenderness ratio

m = slope of the line

P = vertical load applied at midspan (N, kN)

r = radius of gyration (mm)

RT = room temperature (°C)

T = temperature exposure (°C)

T_g = glass transition temperature of the resin matrix (°C)

σ = flexural strength

σ_{Lo} = flexural strength along the pultrusion direction (MPa)

σ_{Lo-RT} = flexural strength along the pultrusion direction at room temperature (MPa)

σ_{Tr} = flexural strength perpendicular to the pultrusion direction (MPa)

σ_{Tr-RT} = flexural strength perpendicular to the pultrusion direction at room temperature (MPa)

Δ = total maximum deflection (mm)

Δ_f = deflection due to flexural deformation (mm)

Δ_{Lo} = total maximum deflection of longitudinally cut specimens (mm)

Δ_s = deflection due to shear deformation (mm)

Δ_{Tr} = total maximum deflection of transversely cut specimens (mm)

Acknowledgement

The authors would like to thank Wagners Composites Fibre Technology (WCFT), Toowoomba, Australia, for providing the test samples.

References

[1] Keller T, Rothe J, De Castro J, Osei-Antwi M. GFRP-balsa sandwich bridge deck: Concept, design, and experimental validation. Journal of Composites for Construction. 2013;18:04013043.
[2] Kumar P, Chandrashekhara K, Nanni A. Testing and evaluation of components for a composite bridge deck. Journal of reinforced plastics and composites. 2003;22:441-61.
[3] Manalo AC, Aravinthan T, Fam A, Benmokrane B. State-of-the-art review on FRP sandwich systems for lightweight civil infrastructure. Journal of Composites for Construction. 2016a:04016068.
[4] Sousa JM, Correia JR, Cabral-Fonseca S, Diogo AC. Effects of thermal cycles on the mechanical response of pultruded GFRP profiles used in civil engineering applications. Composite Structures. 2014;116:720-31.
[5] Correia JR, Bai Y, Keller T. A review of the fire behaviour of pultruded GFRP structural profiles for civil engineering applications. Composite Structures. 2015;127:267-87.
[6] Wong P, Wang Y. An experimental study of pultruded glass fibre reinforced plastics channel columns at elevated temperatures. Composite Structures. 2007;81:84-95.
[7] Bai Y, Keller T, Vallée T. Modeling of stiffness of FRP composites under elevated and high temperatures. Composites Science and Technology. 2008a;68:3099-106.
[8] Bai Y, Post NL, Lesko JJ, Keller T. Experimental investigations on temperature-dependent thermo-physical and mechanical properties of pultruded GFRP composites. Thermochimica Acta. 2008b;469:28-35.
[9] Correia JR, Gomes MM, Pires JM, Branco FA. Mechanical behaviour of pultruded glass fibre reinforced polymer composites at elevated temperature: Experiments and model assessment. Composite Structures. 2013;98:303-13.
[10] Dao M, Asaro RJ. A study on failure prediction and design criteria for fiber composites under fire degradation. Composites Part A: Applied science and manufacturing. 1999;30:123-31.
[11] Dutta PK, Hui D. Creep rupture of a GFRP composite at elevated temperatures. Computers & Structures. 2000;76:153-61.
[12] Mahieux C, Reifsnider K. Property modeling across transition temperatures in polymers: a robust stiffness–temperature model. Polymer. 2001;42:3281-91.
[13] Gibson A, Wu Y-S, Evans J, Mouritz A. Laminate theory analysis of composites under load in fire. Journal of Composite Materials. 2006;40:639-58.
[14] Mahieux C, Reifsnider K, Case S. Property modeling across transition temperatures in PMC's: Part I. Tensile properties. Applied Composite Materials. 2001;8:217-34.
[15] Fan Z, Santare MH, Advani SG. Interlaminar shear strength of glass fiber reinforced epoxy composites enhanced with multi-walled carbon nanotubes. Composites Part A: Applied science and manufacturing. 2008;39:540-54.
[16] Bank LC. Flexural and shear moduli of full-section fiber reinforced plastic (FRP) pultruded beams. Journal of Testing and Evaluation. 1989;17:40-5.

[17] ISO 1172:1996. Textile-glass-reinforced plastics — prepregs, moulding compounds and laminates — determination of the textile-glass and mineral-filler content — calcination methods. International Organization for Standardization. Geneva, Switzerland1996.
[18] ASTM D792. Standard test methods for density and specific gravity (relative density) of plastics by displacement. ASTM International. West Conshohocken, PA2013.
[19] ASTM D790. Standard test methods for flexural properties of unreinforced and reinforced plastics and electrical insulating materials. ASTM International. West Conshohocken, PA2015.
[20] Liu H, Gu Y, Li M, Li Y, Zhang Z. Correlation of temperature dependences of macro-and micro-interfacial properties in carbon fiber/epoxy resin composite. Journal of reinforced plastics and composites. 2012:0731684412467842.
[21] Selmy A, Elsesi A, Azab N, El-baky MA. Interlaminar shear behavior of unidirectional glass fiber (U)/random glass fiber (R)/epoxy hybrid and non-hybrid composite laminates. Composites Part B: Engineering. 2012;43:1714-9.
[22] Chan A, Chiu W, Liu X. Determining the elastic interlaminar shear modulus of composite laminates. Composite Structures. 2007;80:396-408.
[23] Muttashar M, Karunasena W, Manalo A, Lokuge W. Behaviour of hollow pultruded GFRP square beams with different shear span-to-depth ratios. Journal of Composite Materials. 2015:0021998315614993.
[24] Guades E, Aravinthan T, Islam MM. Characterisation of the mechanical properties of pultruded fibre-reinforced polymer tube. Materials & Design. 2014;63:305-15.
[25] Liao K, Schultheisz CR, Hunston DL. Effects of environmental aging on the properties of pultruded GFRP. Composites Part B: Engineering. 1999;30:485-93.
[26] Bai Y, Keller T. Delamination and kink-band failure of pultruded GFRP laminates under elevated temperatures and compression. Composite Structures. 2011;93:843-9.
[27] Manalo AC, Wani E, Zukarnain NA, Karunasena W, Lau K-t. Effects of alkali treatment and elevated temperature on the mechanical properties of bamboo fibre–polyester composites. Composites Part B: Engineering. 2015;80:73-83.
[28] Manalo AC, Surendar S, van Erp G, Benmokrane B. Flexural behavior of an FRP sandwich system with glass-fiber skins and a phenolic core at elevated in-service temperature. Composite Structures. 2016b;152:96-105.
[29] St John NA, Brown JR. Flexural and interlaminar shear properties of glass-reinforced phenolic composites. Composites Part A: Applied science and manufacturing. 1998;29:939-46.
[30] Lahuerta F, Nijssen R, van der Meer F, Sluys L. The influence of curing cycle and through thickness variability of properties in thick laminates. Journal of Composite Materials. 2016:0021998316648758.
[31] Roberts T, Al-Ubaidi H. Flexural and torsional properties of pultruded fiber reinforced plastic I-profiles. Journal of Composites for Construction. 2002;6:28-34.
[32] Neto ABdSS, La Rovere HL. Flexural stiffness characterization of fiber reinforced plastic (FRP) pultruded beams. Composite Structures. 2007;81:274-82.